

Strain effect in a GaAs-In_{0.25}Ga_{0.75}As-Al_{0.5}Ga_{0.5}As asymmetric quantum wire

Y. Fu and M. Willander

Microelectronics Center at Chalmers, Physical Electronics and Photonics, Department of Physics, University of Gothenburg and Chalmers University of Technology, Fysikgränd 3, S-412 96 Gothenburg, Sweden

W. Lu, X. Q. Liu, and S. C. Shen

National Laboratory for Infrared Physics, Shanghai Institute of Technical Physics, Chinese Academy of Sciences, 420 Zhong Shan Bei Yi Road, Shanghai 200083, China

C. Jagadish

Department of Electronic Material Engineering, Research School of Physical Science and Engineering, the Australian National University, Canberra 0200, A.C.T., Australia

M. Gal

School of Physics, University of New South Wales, Sydney, New South Wales 2052, Australia

J. Zou and D. J. H. Cockayne

Electron Microscope Unit and Australian Key Center for Microscopy and Microanalysis, The University of Sydney, NSW 2006, Australia

(Received 21 October 1998; revised manuscript received 24 August 1999)

We report a theoretical investigation of the strain effects on the electronic energy band in a GaAs-In_{0.25}Ga_{0.75}As-Al_{0.5}Ga_{0.5}As asymmetric quantum wire formed in a V-grooved substrate. Our model is based on the sp^3s^* tight-binding model. It includes different spatial distributions of the lattice-mismatch-induced strain. We solve numerically the tight-binding Hamiltonian through the local Green's function from which the electronic local density of states (LDOS) is obtained. The detailed energy band structure (discrete localized states and energy bands of extended states) and the spatial distribution of the eigenfunctions (wave function amplitude of nondegenerate states or sum of the wave function amplitudes of degenerate states) are directly reflected in the LDOS. Spatial mapping of the LDOS's shows a reduction of the lowest excitation energies in different regions of the system when the local lattice structure of the In_{0.25}Ga_{0.75}As layer relaxes from completely strained to completely relaxed. By comparing the calculated results with photoluminescence measurement data, we conclude that the strain in the In_{0.25}Ga_{0.75}As layer relaxes linearly from the heterointerface with the Al_{0.5}Ga_{0.5}As buffer layer to the heterointerface with the top GaAs layer.

I. INTRODUCTION

The great success in confining electrons in two-dimensional (2D) quantum wells^{1,2} has excited further interest in even lower-dimensional systems, i.e., quasi-one-dimensional^{3,4} (1D) and quasi-zero-dimensional (0D) semiconductors.⁵ Compared with bulk semiconductor materials, low-dimensional semiconductor systems are expected to have superior properties for optoelectronic device applications.^{6,7} The recently fabricated quantum wire (QWR) lasers^{3,4} have shown a large reduction of the threshold current density and enhancements of the gain and bandwidth.

Energy band engineering techniques are very important for device performance optimization in electronics as well as optoelectronics. In addition to the normal heterointerface construction, the strain effect induced by lattice mismatch between heteromaterials is an extra physical parameter in modifying the energy band structure of the heterostructure, e.g., a 2D quantum well.⁸ Similar results can also be expected for quantum wires. GaAs-In_yGa_{1-y}As pseudomorphic QWRs have been successfully fabricated and applied as laser-active materials.⁴ Both the In composition and the thickness of the active In_yGa_{1-y}As layer can be modified to

tailor the energy band structure of the system.

However, the variation in the In composition and the layer thickness are limited by the critical thickness of the strain due to the lattice mismatch.^{9,10} When an Al_xGa_{1-x}As layer is used as the quantum barrier in the pseudomorphic system, we can utilize the Al composition as another parameter for energy band engineering without much change in the amount of lattice mismatch in the In_yGa_{1-y}As layer. For example, the range of variation in barrier height can be further extended. Such an Al_xGa_{1-x}As-In_yGa_{1-y}As QWR grown on a V-groove GaAs(100) substrate has been experimentally fabricated¹¹ and theoretically studied.¹²

Most theoretical works are based on the effective-mass approximation for quantum wires.¹³⁻¹⁷ A $\mathbf{k}\cdot\mathbf{p}$ approximation together with the deformation Hamiltonian of Pikus and Bir¹⁸ has been extensively applied.^{12,19} Because of the complicated strain situations and the relatively small spatial extensions of the quantum wire and quantum well regions, we apply here the sp^3s^* tight-binding model²⁰ to describe the energy band structure of the quantum wire system. The problems concerning the validity of the $\mathbf{k}\cdot\mathbf{p}$ approximation and the strain Hamiltonian developed for bulk materials can thus be avoided.

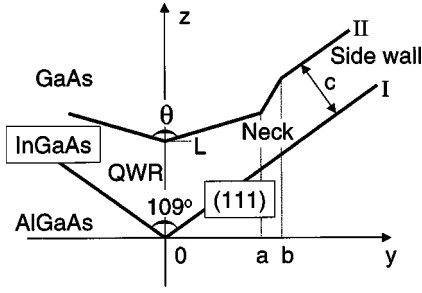


FIG. 1. Geometric structure of the Al_{0.5}Ga_{0.5}As-In_{0.25}Ga_{0.75}As-GaAs quantum wire. $L = 12$, $a = 32$, $b = 36$, $c = 5.5$ nm, $\theta = 135^\circ$.

We describe briefly the sample fabrication and characterization in Sec. II. The sp^3s^* tight-binding model is introduced in Sec. III, where the model Hamiltonian is numerically solved through the local Green's function, from which the local density of states is obtained. Experimental results and theoretical analysis of the energy band structure of the quantum wire system are presented in Sec. IV. A brief summary is made in Sec. V.

II. EXPERIMENTAL RESULTS

The QWR sample under investigation in this work is V shaped. We processed the GaAs(100) semi-insulating substrate by standard photolithography and wet etching. A mask with 50 stripes, each 2 μm wide and with 2 μm spacing in between, was used to obtain V grooves with a period of 4 μm . The patterned wafer was selectively etched with $\text{H}_2\text{O}:\text{H}_2\text{O}_2:\text{H}_3\text{PO}_4(1:1:3)$ at 0 $^\circ\text{C}$ and V grooves were formed by the two (111) surfaces. The V grooved substrate was then cleaned with acetone, methanol, and deionized (DI) water and the trim etching was accomplished with $\text{H}_2\text{SO}_4:\text{H}_2\text{O}_2:\text{H}_2\text{O}(20:1:1)$. After being rinsed with DI water and blown dry with pure N_2 , the wafer was loaded into a low-pressure metal-organic-chemical deposition reactor to grow a 0.1- μm -thick GaAs buffer layer followed by a 1- μm -thick Al_{0.5}Ga_{0.5}As layer. Both layers were grown at 750 $^\circ\text{C}$. Finally a 3-nm In_{0.25}Ga_{0.75}As wire layer was deposited, followed by a 0.1- μm -thick GaAs top barrier layer at 700 $^\circ\text{C}$.

The cross section of the Al_{0.5}Ga_{0.5}As-In_{0.25}Ga_{0.75}As-GaAs quantum wire sample was studied by transmission electron microscopy (TEM) and is schematically presented in Fig. 1. Parameters in Fig. 1 are derived from the TEM measurement. Optical properties of the QWR sample were studied by photoluminescence (PL). The sample was cooled down in a He-recycled cryogenic dewar to a temperature of 8 K with a He-Ne laser 543 nm line as excitation source. A Si charge-coupled device was used as the detector through a 0.25 m monochromator. The resulting PL spectrum is presented in Fig. 2. From the PL spectrum and the fitting process, four PL peaks, A = 1.356 eV, B = 1.413 eV, C = 1.441 eV, and D = 1.464 eV, are clearly resolved. They were denoted as originating from the QWR, the sidewall quantum well (QW), the neck region, and the top GaAs layer, respectively.²¹

Because of the 1 μm Al_{0.5}Ga_{0.5}As layer between the substrate and the In_{0.25}Ga_{0.75}As layer, we are not able to observe a PL signal from the GaAs substrate due to the high absorption rate in the Al_{0.5}Ga_{0.5}As layer. Moreover, most carriers quickly relax to low-energy states before radiative

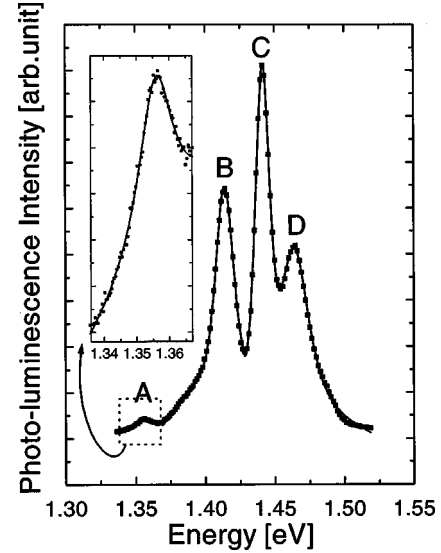


FIG. 2. Photoluminescence spectrum (dots) at 8 K. The spectrum is fitted by a Lorentzian and Gaussian mixed line shape (solid lines).

transitions in the Al_{0.5}Ga_{0.5}As layer, so that we are not able to observe the PL signal from the Al_{0.5}Ga_{0.5}As layer either. However, a weak PL peak at 1.520 eV is observed experimentally, which is related to the bulk GaAs substrate.

III. PHYSICAL MODEL FOR THE STRAIN EFFECT

To study the electron energy band structure of the Al_xGa_{1-x}As-In_yGa_{1-y}As-GaAs QWR shown in Fig. 1, we apply the well-established sp^3s^* tight-binding model of Vogl, Hjalmarson, and Dow.²⁰ The model was developed from Harrison's sp^3 tight-binding model²² and has been successfully applied to many semiconductor materials, e.g., in Ref. 23. Five Löwdin orbitals, $|s\rangle$, $|p_x\rangle$, $|p_y\rangle$, $|p_z\rangle$, and $|s^*\rangle$, are introduced in the model at each atomic site \mathbf{r}_i . The matrix element of the tight-binding Hamiltonian is denoted as $h(\alpha\beta, ij)$ between the α th orbital on the i th atomic site $|\alpha, i\rangle$ and the β th orbital on the j th site $|\beta, j\rangle$, where either $i = j$ or i is a nearest neighbor of j . These matrix elements are listed in Table I obtained from Ref. 20. Here the diagonal elements are denoted as E (orbital energies), and the off-diagonal elements are V (interaction energies).

In Ref. 20, the top of the valence band, $\Gamma_{15}^v = 0$, is used as the reference energy for every individual element or compound semiconductor material. To calculate the energy band structures of alloys or heteromaterials, the absolute positions of Γ_{15}^v for the compositional materials need to be determined before applying the sp^3s^* tight-binding theory. It has been observed experimentally that referred to GaAs Γ_{15}^v , a valence band offset $\Delta E_v = \Gamma_{15}^v(\text{AlAs}) = -0.4$ eV is obtained for AlAs by fitting the calculated band gap of an Al_xGa_{1-x}As alloy²⁴ with the experimental data of Refs. 25 and 26. A valence band offset of -0.5 eV was obtained when fitting the measurement data of Ref. 27. We adopt a valence band offset of -0.4 eV (Ref. 28) in this work.

The ratio between the conduction/valence band offset and the energy band gap difference is normally defined as the conduction/valence band offset coefficient when studying

TABLE I. Energy band structure parameters for the sp^3s^* tight-binding band calculation.

	AlAs	InAs	GaAs
$E(s,a)$	-7.5273	-9.5381	-8.3431
$E(p,a)$	0.9833	0.9099	1.0414
$E(s^*,a)$	7.4833	7.4099	8.5914
$E(s,c)$	-1.1627	-2.7219	-2.6569
$E(p,c)$	3.5867	3.7201	3.6686
$E(s^*,c)$	6.7267	6.7401	6.7386
$V(s,s)$	-6.6642	-5.6052	-6.4513
$V(x,x)$	1.8780	1.8398	1.9546
$V(x,y)$	4.2919	4.4693	5.0779
$V(sa,pc)$	5.1106	3.0354	4.4800
$V(sc,pa)$	5.4965	5.4389	5.7839
$V(s^*a,pc)$	4.5216	3.3744	4.8422
$V(pa,s^*c)$	4.9950	3.9097	4.8077
ΔE_v	0.4	0.1	0.0
a (Å)	5.6533 (Ref. 32)	6.0583 (Ref. 29)	5.6611 (Ref. 33)

heteromaterials. A valence band offset coefficient of 0.3 is usually accepted for a lattice-matched $\text{In}_{0.53}\text{Ga}_{0.47}\text{As}-\text{In}_{0.52}\text{Al}_{0.48}\text{As}$ system, indicating a valence band offset of 0.225 eV for such a system.^{29,30} By applying the same numerical method of energy band structure calculations for compositionally random $\text{In}_{0.53}\text{Ga}_{0.47}\text{As}$ and $\text{In}_{0.52}\text{Al}_{0.48}\text{As}$ alloys as in our earlier work,²⁴ we have obtained a valence band offset of 0.1 eV for InAs with respect to GaAs, in good agreement with experimental data of 0.1 ± 0.07 eV (Ref. 28) and 0.17 eV.³¹

The lattice constants of AlAs, InAs, and GaAs bulk materials are 5.6533,³² 6.0583,²⁹ and 5.6611 Å,³³ respectively.

We now determine the interactions between atoms in the heteromaterial lattice. We first determine the local atomic bond lengths. The local atomic bond lengths depend on the distribution of the four types of atoms in the system. The anion lattice sites are occupied by As atoms. We assume in the present study that the cation lattice sites in $\text{Al}_x\text{Ga}_{1-x}\text{As}$ and $\text{In}_y\text{Ga}_{1-y}\text{As}$ layers are randomly occupied (determined by random number generation in the computer) by Al, Ga, and In atoms according to their corresponding mole contents. (Further work to include the short-range- and long-range-order effects²⁴ can be performed in a similar manner.) The atomic bond lengths between atoms in the $\text{Al}_x\text{Ga}_{1-x}\text{As}$ region are obtained by linear interpolation between atomic bond lengths in bulk GaAs and AlAs in the form of Vegard's law:

$$a_{\text{AlGaAs}} = xa_{\text{AlAs}} + (1-x)a_{\text{GaAs}}. \quad (1)$$

For the $\text{In}_y\text{Ga}_{1-y}\text{As}$ layer grown on the V-grooved $\text{Al}_x\text{Ga}_{1-x}\text{As}$ layer, we consider two extreme strain situations in this work: (a) the $\text{In}_y\text{Ga}_{1-y}\text{As}$ layer is completely strained, having the lattice constant of a_{AlGaAs} ; (b) the $\text{In}_y\text{Ga}_{1-y}\text{As}$ layer is completely relaxed and

$$a_{\text{InGaAs}} = ya_{\text{InAs}} + (1-y)a_{\text{GaAs}}. \quad (2)$$

In this case, the top GaAs layer is then strained as it is grown on the relaxed $\text{In}_y\text{Ga}_{1-y}\text{As}$ QWR layer. The real strain dis-

tribution in the $\text{GaAs}-\text{In}_y\text{Ga}_{1-y}\text{As}-\text{Al}_x\text{Ga}_{1-x}\text{As}$ QWR system lies between these two cases. The strain can also be spatially distributed; it is greater in the region close to the $\text{Al}_x\text{Ga}_{1-x}\text{As}$ layer and relaxed close to the GaAs layer.

Knowing the local bond lengths, the interaction matrix elements for strained GaAs, $\text{In}_y\text{Ga}_{1-y}\text{As}$, and $\text{Al}_x\text{Ga}_{1-x}\text{As}$ layers are determined by the well-known d^{-2} scaling rule.^{22,34}

Thus far we have specified all the necessary physical parameters for the Löwdin orbitals in the $\text{GaAs}-\text{In}_y\text{Ga}_{1-y}\text{As}-\text{Al}_x\text{Ga}_{1-x}\text{As}$ system. The eigenfunction of the system is expressed as

$$\sum_{\alpha,i} C(\alpha,i)|\alpha,i\rangle,$$

where the coefficients in the above linear combination satisfy the eigenvalue equation

$$\sum_{\beta,j} h(\alpha\beta,ij)C(\beta,j) = EC(\alpha,i). \quad (3)$$

Since the system lacks the translational symmetry that is the base for wave function expansion in \mathbf{k} space, the above equation has to be solved in real space. Many numerical methods have been developed to study electronic energy band structure in real space. Among them is the recursion method developed by Haydock, Heine, and Kelly³⁵ which is well suited for the study of local environment effects here. The recursion method constructs a new set of normalized orthogonal base functions, in which the general Hamiltonian matrix is converted into a tridiagonal form. The diagonal elements $g(\mathbf{r}_i, E)$ of the corresponding Green's function at \mathbf{r}_i are expressed as continued fractions of the diagonal and off-diagonal elements of the tridiagonalized Hamiltonian matrix, from which the local densities of states (LDOSs) are obtained.

More specifically, we construct a base from

$$|1\rangle = \begin{pmatrix} \vdots \\ 0 \\ 1 \\ 0 \\ \vdots \end{pmatrix} \cdots \begin{pmatrix} i-1 \\ i \\ i+1 \end{pmatrix}, \quad (4)$$

and $|2\rangle$ and higher states $|n\rangle$ are defined by

$$|2\rangle = H|1\rangle - a_1|1\rangle,$$

...

$$|n+1\rangle = H|n\rangle - a_n|n\rangle - b_{n-1}^{1/2}|n-1\rangle, \quad (5)$$

where

$$a_n = \frac{\langle n|H|n\rangle}{\langle n|n\rangle}, \quad b_{n-1} = \frac{\langle n|n\rangle}{\langle n-1|n-1\rangle}. \quad (6)$$

The local Green's function and the local density of states at \mathbf{r}_i are expressed as

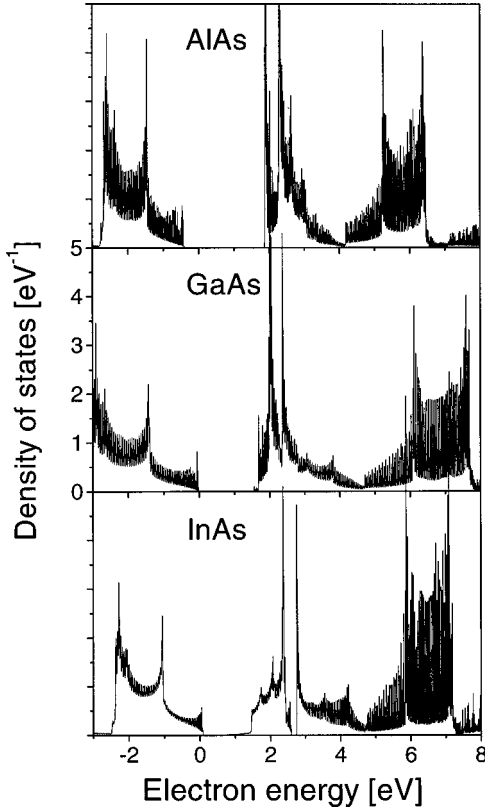


FIG. 3. Electronic densities of states of bulk AlAs, GaAs, and InAs.

$$g(\mathbf{r}_i, E) = \frac{1}{E - a_1 - \frac{b_1}{E - a_2 - \frac{b_2}{E - a_3 - \dots}}},$$

$$\nu(\mathbf{r}_i, E) = -\frac{1}{\pi} \lim_{\beta \rightarrow 0} \{\text{Im}[g(\mathbf{r}_i, E + i\beta)]\}. \quad (7)$$

The local density of states at different atomic sites is easily obtained by modifying $i(\mathbf{r}_i)$ in Eq. (4) across the system (or part of the system under investigation).

From the theory of the Green's function,³⁶ we know that the local density of states is the sum of the amplitudes of degenerate wave functions at E :

$$\nu(\mathbf{r}_i, E) = \sum_{nm} |\psi_{nm}(\mathbf{r}_i)|^2 \delta_{E, E_n}, \quad (8)$$

where E_n is the n th energy state and m is the index of degenerate states at E_n . It is then understood that in the case of a nondegenerate eigenstate the LDOS represents the spatial distribution of the eigenwave function. For degenerate states, integration of the LDOS over the whole space gives us the number of states at E (the degeneracy). In both cases the LDOS gives us the spatial distribution of carrier(s) at a certain energy level. Complicated as a way to solve numerically the multiple-dimensional Schrödinger equation, the recursion method is a relatively simple way to obtain the energy band structure and spatial carrier distribution. While the LDOS

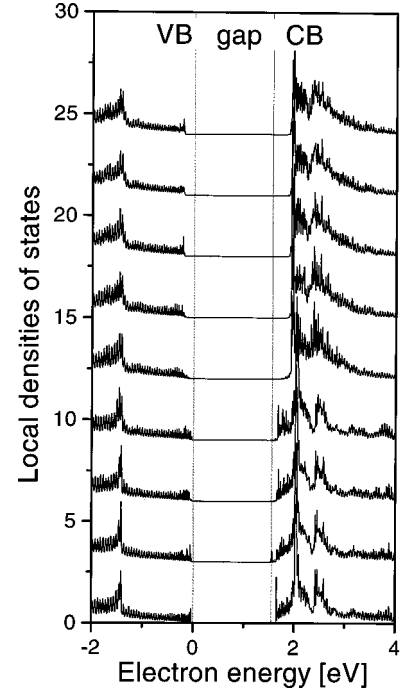


FIG. 4. Local densities of states of the completely strained quantum wire. $x=y=0$. From the bottom to the uppermost LDOS, $z = 5.6, 4.2, 2.8, 1.4, 0, -1.4, -2.8, -4.2, -5.6$ nm. VB is the valence band, CB the conduction band.

does not contain phase information for the wave function, it provides us with a set of nondegenerate states and the band edges of continuous energy bands which can be compared directly with the PL spectrum. The method has been successfully applied to various systems.^{23,37}

In Fig. 3 we present the calculated densities of states of crystalline AlAs, InAs, and GaAs using an atomic cluster containing 1 500 000 atoms. The computer RAM requirement for such a cluster is about 250 megabytes, the upper limit of our computation capability. As the size of the atom cluster is limited, we have applied the numerical method discussed in Ref. 37 to expand the number of diagonal and off-diagonal elements of the tridiagonalized Hamiltonian.

IV. RESULT ANALYSIS AND DISCUSSION

Figure 4 shows the calculated LDOS's in the quantum wire region along the z axis. Here the whole system assumes the lattice constant of the Al _{x} Ga _{$1-x$} As layer so that the In _{y} Ga _{$1-y$} As layer is completely strained; the top GaAs layer is slightly strained due to the small difference between the AlAs and GaAs lattice constants. We have observed the LDOS of the Al _{x} Ga _{$1-x$} As alloy deep in the Al _{x} Ga _{$1-x$} As layer ($z < -2$ nm). On gradually moving into the quantum wire region, we have obtained LDOS's very similar to that of the bulk GaAs material. We do not see any sign of the LDOS of the In _{y} Ga _{$1-y$} As alloy. The result is similar to that in the Si _{$1-y$} C _{y} system.²³ Since the modification of the energy band structure by the strain is described by the general d^{-2} scaling law, the overall interaction strengths of the In-As bonds in the InAs layer, which have a crystal Ga-As bond length, are closer to those of Ga-As than to those in crystalline InAs (the "universal" model, see Refs. 20,38). Thus, the LDOS in the

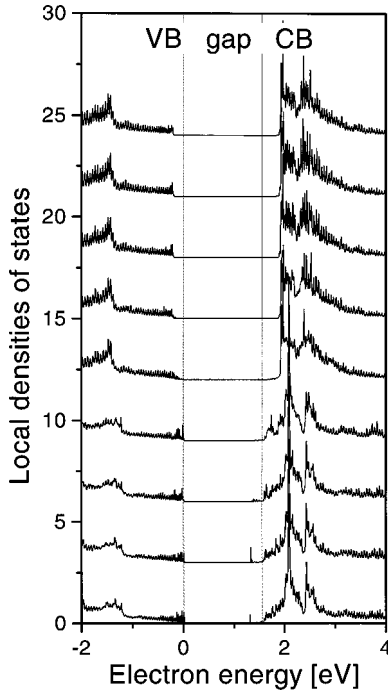


FIG. 5. Same as Fig. 4 but for a completely relaxed quantum wire system.

$\text{In}_y\text{Ga}_{1-y}\text{As}$ region is now transferred from that of the strain-free $\text{In}_y\text{Ga}_{1-y}\text{As}$ alloy to that of bulk GaAs by the strain.

The valence band edge is not much affected by the heterostructure due to the small band offset between GaAs and $\text{In}_{0.25}\text{Ga}_{0.75}\text{As}$ (small quantum confinement). The lowest-energy state in the conduction band is 1.526 eV. Since the energy band gap of crystalline GaAs is 1.550 eV from the present sp^3s^* tight-binding model, we deduce a lowest excitation energy of only 0.024 eV less than the GaAs band gap, much smaller than the measured value of $1.520 - 1.356 = 0.164$ eV at 8 K [the measured GaAs band gap is 1.520 eV (Ref. 39)]. We have to conclude that the $\text{In}_y\text{Ga}_{1-y}\text{As}$ layer is not likely to be completely strained.

When all atomic bonds in the system become totally relaxed and have the bond lengths of the corresponding bulk crystals, the LDOS's are very different. In Fig. 5, we observe localized valence band and conduction band sublevels. The two ground sublevels at 0.021 and 1.297 eV give us a lowest excitation energy of $1.297 - 0.021 = 1.276$ eV, which is 0.274 eV below the GaAs band gap of 1.550 eV. This value is larger than the experimental value of 0.164 eV.

The LDOS'S and the excitation energies (with respect to the GaAs band gap) in the neck region and the sidewall quantum well region have also been calculated in a similar way for both the completely strained and relaxed situations. For a completely strained lattice, the lowest excitation energies below the GaAs band gap in the two regions are 0.015 and 0.040 eV, respectively, much smaller than those (0.079 and 0.107 eV) observed in the PL spectrum. They are 0.097 and 0.130 eV, respectively, when the lattice becomes completely relaxed.

We have listed the PL peak positions and the calculated excitation energies in Table II. As the PL excitation energies are in the theoretical range determined by the completely strained and completely relaxed cases, it is to be concluded

TABLE II. Excitation energies below the bulk GaAs band gap (eV).

	A	B	C	D
Measured	0.164	0.107	0.079	0.056
Strained	0.024	0.040	0.015	0.00
Relaxed	0.274	0.130	0.097	0.097
Strain-relax	0.120	0.092	0.065	0.049

that the strain in the $\text{In}_y\text{Ga}_{1-y}\text{As}$ layer is spatially distributed. Close to the $\text{Al}_x\text{Ga}_{1-x}\text{As}$ layer the $\text{In}_y\text{Ga}_{1-y}\text{As}$ layer is strained, while close to the top GaAs layer it becomes relaxed.

We have modified the computer-simulated lattice structure so that the lattice constant in the $\text{In}_y\text{Ga}_{1-y}\text{As}$ region is relaxed linearly from a_{AlGaAs} at surface I in Fig. 1 to a_{InGaAs} at surface II (strain-relax case in Table II. The top GaAs layer is strained in this case as it is grown on the relaxed $\text{In}_y\text{Ga}_{1-y}\text{As}$ layer. The calculated LDOS in the $\text{In}_y\text{Ga}_{1-y}\text{As}$ region close to the top GaAs layer ($z = 10.6$ nm, $x = y = 0$) shows the lowest excitation energy of 0.120 eV below the GaAs energy band gap, which is very close to the measured value of 0.164 eV.

The excitation energies with respect to the GaAs band gap in the neck region and the sidewall quantum well regions are 0.065 and 0.092 eV, respectively, in the situation when the strain in the $\text{In}_y\text{Ga}_{1-y}\text{As}$ is distributed linearly from surface I to surface II.

We now try to identify PL peak D which is normally attributed to the top GaAs layer. From Figs. 4 and 5 we can see that the energy band gap in the slightly strained GaAs top layer is basically zero, while it is reduced by tensile strain when a GaAs layer is grown on the relaxed $\text{In}_y\text{Ga}_{1-y}\text{As}$ layer. The reduction is about 0.097 eV. We identify this as the origin of the experimentally observed PL peak D. When the $\text{In}_y\text{Ga}_{1-y}\text{As}$ layer relaxes linearly from surface I to II, the excitation energy becomes 0.049 eV below the GaAs band gap.

Before the final conclusion, let us discuss the starting point of the present investigation. As discussed in our earlier work,²³ simple as is the sp^3s^* tight-binding model adopted in this work, the qualitative conclusions about the energy band structure of our QWR system and the spatially distributed strain are derived from the general d^{-2} scaling rule. Extended tight-binding models can improve the quantitative results, e.g., the GaAs band gap; the qualitative conclusions remain unchanged, however.

The second thing to be carefully examined is the LDOS calculation method. As briefly mentioned earlier, the recursion method transfers the general Hamiltonian into a tridiagonalized matrix. Since theoretically the system under investigation is infinitely extended in the yz plane and numerically we are not able to find all the diagonal and off-diagonal elements in the tridiagonalized matrix, the local Green's function is approximated by artificially extrapolating the diagonal and off-diagonal elements based on their oscillation properties. If not properly treated, such an approximation can easily result in false LDOS's in the continuous energy bands that correspond to spatially extended states. In fact, we really observe rapid oscillations in the LDOS in continuous energy bands in Figs. 3–5. However, discrete energy levels (spa-

tially localized states, especially low-lying states like the ground state) are less affected by the boundary conditions used in the recursion method. These are actually the states we are much concerned with, as listed in Table II in the present study.

V. CONCLUSION

In a brief summary we report on the successful fabrication of an In_yGa_{1-y}As QWR grown on the V-groove Al_xGa_{1-x}As-GaAs (100) substrate. Theoretical investigations of the electronic energy band structure of the system are conducted using the sp^3s^* tight-binding model with which the lattice-mismatch-induced strain effect can easily be coupled.

We have solved the tight-binding Hamiltonian numeri-

cally via the local Green's function from which the electronic local densities of states have been derived. The local density of states is the sum of the wave function amplitudes of degenerate states. It represents the spatial distribution of an electron at a certain energy level. Discrete energy states confined in the QWR region and energy bands of extended states over the barrier height are clearly reflected in the LDOS and are readily comparable with the PL spectrum. We have carefully examined the electronic energy band structures in the presence of a spatially distributed lattice-mismatch-induced strain in the In_yGa_{1-y}As QWR. By combining the PL spectrum with the calculated LDOS spectra we have concluded that in our V-grooved GaAs-In_{0.25}Ga_{0.75}As-Al_{0.5}Ga_{0.5}As asymmetric QWR, the strain is rather strong in the In_{0.25}Ga_{0.75}As layer and is spatially distributed.

-
- ¹L. Esaki and R. Tsu, IBM J. Res. Dev. **14**, 61 (1970).
²B. F. Levine, J. Appl. Phys. **74**, R1 (1993).
³E. Kapon, D. M. Hwang, and R. Bhat, Phys. Rev. Lett. **63**, 430 (1989).
⁴M. Walther, E. Kapon, C. Caneau, D. M. Hwang, and L. M. Schiavone, Appl. Phys. Lett. **62**, 2170 (1992).
⁵M. A. Kastner, Phys. Today **46**, 24 (1993).
⁶D. A. B. Miller, D. S. Chemla, and S. Schmitt-Rink, Appl. Phys. Lett. **52**, 2154 (1988).
⁷Y. Arakawa and A. Yariv, IEEE J. Quantum Electron. **22**, 1887 (1986).
⁸E. Kapon, D. M. Hwang, M. Walther, R. Bhat, and N. G. Stoffel, Surf. Sci. **267**, 539 (1992).
⁹M. Gal, P. C. Taylor, B. F. Usher, and P. J. Orders, J. Appl. Phys. **62**, 3898 (1987).
¹⁰T. G. Anderson, Z. G. Chen, V. D. Kulakovskii, A. Uddin, and J. T. Vallin, Appl. Phys. Lett. **51**, 752 (1987).
¹¹W. Lu, Proc. SPIE **3553**, 48 (1998).
¹²M. Grundmann, O. Stier, and D. Bimberg, Phys. Rev. B **50**, 14 187 (1994); O. Stier and D. Bimberg, *ibid.* **55**, 7726 (1997).
¹³K. Chang and J. B. Xia, Phys. Rev. B **58**, 2031 (1998).
¹⁴T. Inoshita and H. Sakaki, J. Appl. Phys. **79**, 269 (1996).
¹⁵D. Gershoni, H. Temkin, G. J. Dolan, J. Dunsmuir, S. N. G. Chu, and M. B. Panish, Appl. Phys. Lett. **53**, 995 (1988).
¹⁶G. Goldoni, F. Rossi, E. Molinari, A. Fasolino, R. Rinaldi, and R. Cingolani, Appl. Phys. Lett. **69**, 2965 (1996).
¹⁷F. Rossi and E. Molinari, Phys. Rev. Lett. **76**, 3642 (1996); Phys. Rev. B **53**, 16 462 (1996).
¹⁸G. E. Pikus and G. L. Bir, Fiz. Tverd. Tela (Leningrad) **1**, 1642 (1959) [Sov. Phys. Solid State **1**, 1502 (1959)].
¹⁹J. Hammersberg, Ph.D. thesis, Department of Physics and Measurement Technology, Linköping University, Sweden, 1998.
²⁰P. Vogl, H. P. Hjalmarson, and J. D. Dow, J. Phys. Chem. Solids **44**, 365 (1983).
²¹Y. Kim, S. Yuan, R. Leon, C. Jagadish, M. Gal, M. B. Johnston, M. R. Phillips, M. A. S. Kalceff, J. Zou, and D. J. H. Cockayne, J. Appl. Phys. **80**, 5014 (1996).
²²W. A. Harrison, *Electronic Structure and the Properties of Solids* (Freeman, San Francisco, 1980).
²³Y. Fu, M. Willander, P. Han, T. Matsuura, and J. Murota, Phys. Rev. B **58**, 7717 (1998).
²⁴Y. Fu, K. A. Chao, and R. Osorio, Phys. Rev. B **40**, 6417 (1989).
²⁵A. C. Gossard, P. M. Petroff, W. Wiegmann, R. Dingle, and A. Savage, Appl. Phys. Lett. **29**, 323 (1976).
²⁶B. A. Vojak, W. D. Laidig, N. Holonyak, M. D. Camras, J. J. Coleman, and P. D. Dapkus, J. Appl. Phys. **52**, 621 (1981).
²⁷W. I. Wang, Solid-State Electron. **29**, 133 (1986).
²⁸J. M. Moison, C. Guille, M. van Rompay, F. Barthe, F. Houzay, and M. Bensoussan, Phys. Rev. B **39**, 1772 (1989).
²⁹*Properties of Lattice-Matched and Strained InGaAs*, edited by P. Bhattacharya (INSPEC, London, 1993).
³⁰Y. Fu, J. Stake, L. Dillner, M. Willander, and E. L. Kollberg, J. Appl. Phys. **82**, 5568 (1997).
³¹A. D. Katnami and R. S. Bauer, Phys. Rev. B **33**, 1106 (1986).
³²C. M. H. Driscoll, A. F. W. Willoughby, J. B. Mullin, and B. W. Straughan, *Gallium Arsenide and Related Compounds* (Institute of Physics, London, 1975), p. 275.
³³J. Whitaker, Solid-State Electron. **8**, 649 (1965).
³⁴J. C. Slater and G. F. Koster, Phys. Rev. **94**, 1498 (1954).
³⁵R. Haydock, V. Heine, and M. J. Kelly, J. Phys. C **5**, 2845 (1972).
³⁶E. N. Economons, in *Green's Function in Quantum Physics*, edited by M. Cardona (Springer-Verlag, Berlin, 1979).
³⁷*The Recursion Method and Its Application*, edited by D. G. Pettifor and D. L. Weaire (Springer-Verlag, Berlin, 1985).
³⁸D. Pettifor, *Bonding and Structure of Molecules and Solids* (Clarendon, Oxford, 1995).
³⁹S. M. Sze, *Physics of Semiconductor Devices* (Wiley, New York, 1981).